# A Potential Field-Based Model Predictive Path-Planning Controller for Autonomous Road Vehicles

Yadollah Rasekhipour, Amir Khajepour, Shih-Ken Chen, and Bakhtiar Litkouhi

***Abstract*—Artificial potential fields and optimal controllers are two common methods for path planning of autonomous vehicles. An artificial potential field method is capable of assigning different potential functions to different types of obstacles and road structures and plans the path based on these potential functions. It does not, however, include the vehicle dynamics in the path-planning process. On the other hand, an optimal path-planning controller integrated with vehicle dynamics plans an optimal feasible path that guarantees vehicle stability in following the path. In this method, the obstacles and road boundaries are usually included in the optimal control problem as constraints and not with any arbitrary function. A model predictive path-planning controller is introduced in this paper such that its objective includes potential functions along with the vehicle dynamics terms. Therefore, the path-planning system is capable of treating different obstacles and road structures distinctly while planning the optimal path utilizing vehicle dynamics. The path-planning controller is modeled and simulated on a CarSim vehicle model for some complicated test scenarios. The results show that, with this path-planning controller, the vehicle avoids the obstacles and observes road regulations with appropriate vehicle dynamics. Moreover, since the obstacles and road regulations can be defined with different functions, the path-planning system plans paths corresponding to their importance and priorities.**

***Index Terms*—Path planning, autonomous vehicles, road vehicles, model predictive control, artificial potential field, vehicle dynamics and control.**

## I. Introduction

A LARGE percentage of car accidents is caused by driver errors [1]. A fully autonomous driving could reduce such accidents significantly. Besides, it increases the comfort of traveling by obviating the need for a driver. However, if it is intended to replace a driver, an autonomous system should be intelligent enough to handle different driving scenarios for various obstacles and road regulations. Planning the vehicle's path based on road regulations and obstacles is performed in the path planning module of an autonomous vehicle. Developing such a module so that it is able to plan an appropriate path for any combination of obstacles and road structures is an ongoing research subject.

Path planning has been widely studied in robotics for obstacle avoidance [2]–[4]. For autonomous road vehicles, road structures and regulations should also be considered in the path planning in addition to obstacles. Moreover, considering the vehicle dynamics and tires' and actuators' limitations at the path planning level makes the planned path more feasible to be tracked by the vehicle. The main advanced path planning methods developed for autonomous road vehicles are artificial potential field methods, random search methods, and optimal control methods.

Artificial potential field method generates a potential field based on Potential Functions (PFs) of obstacles, road structures, and goal. It plans the path by moving in the descent direction of the field. Then, a path tracking module calculates the vehicle inputs required to track the path [5], [6]. The main advantage of this method over the other path planning methods is its low calculation cost even with complex PFs for obstacles and road structures. Considering vehicle dynamics in the path tracking module improves the ability of the vehicle in tracking the path. Jie *et al.* [7] introduces a model predictive path tracking controller to consider the vehicle dynamics and actuators' limitations in its path tracking. However, it is possible that the planned path is not feasible to be tracked by the vehicle since the vehicle dynamics and its limitations are not considered in path generation [8]. Noto *et al.* [9] considers the vehicle dynamics in generating the reference path. To plan the path, it calculates steering angle commands that move the vehicle in the potential field descent direction and satisfy the vehicle's dynamics constraints. It then, uses a path tracking controller to follow the planned path. Although it finds a path satisfying the vehicle dynamics, the path is not the optimal path in terms of vehicle dynamics.

Optimal controllers are also used for path planning on structured roads. The approach for considering obstacles in a two dimensional space for obstacle avoidance is a challenge for this path planning method. Shildbach *et al.* [10] designs a scenario-based model predictive controller with two levels. The higher level module determines the reference lane and speed by calculating a time-to-lane-change. At the lower level, the model

Manuscript received March 1, 2016; revised June 3, 2016, July 25, 2016, and August 15, 2016; accepted August 20, 2016. Date of publication September 26, 2016; date of current version May 1, 2017. This work was supported in part by the Automotive Partnership Canada, by the Ontario Research Fund, and by General Motors Company. The Associate Editor for this paper was J. Ploeg.

Y. Rasekhipour and A. Khajepour are with University of Waterloo, Waterloo, ON N2L 3G1, Canada (e-mail: yrasekhi@uwaterloo.ca; akhajepour@uwaterloo.ca).

S.-K. Chen and B. Litkouhi are with General Motors Company, Warren, MI 48090 USA (e-mail: shih-ken.chen@gm.com; bakhtiar.litkouhi@gm.com).

Color versions of one or more of the figures in this paper are available online at http://ieeexplore.ieee.org.

Digital Object Identifier 10.1109/TITS.2016.2604240

predictive controller tracks the reference lane and speed and keeps the vehicle at the safe distance from the obstacles by staying in the safe interval of the reference lane. Carvalho *et al.* [11] calculates the Signed Distance (SD) between the vehicle and an obstacle and generates an approximate linear constraint based on this distance for obstacle avoidance. The predicted obstacles and their corresponding constraints are probabilistic. The road structure is also considered as constraints on the vehicle position. A chance-constrained model predictive controller is used to solve the problem in two dimensions. Carvalho *et al.* [12] considers different vehicle models, driver models, and environment models to simulate different optimal control path planning methods in [10] and [11]. It also simulates a tube-based model predictive controller introduced in [13] for obstacle avoidance in an unstructured path. The method considers the obstacles as ellipse-shaped constraints and keeps the vehicle robustly far from the obstacle while following a desired path by solving a nonconvex optimal control problem. Gao *et al.* [14] includes obstacle avoidance costs in the cost function of a model predictive path planning controller. The obstacle avoidance cost is calculated for each obstacle as a function of the longitudinal distance from the vehicle to the obstacle and whether the obstacle is in the sight of the vehicle. The model predictive controller is nonlinear to solve the two-dimensional obstacle avoidance problem with this obstacle avoidance cost. Moreover, the optimal control problem considers all the obstacles with the same function and does not include road regulations.

In this paper, a model predictive controller is developed for path planning of autonomous vehicles which avoids obstacles and observes road regulations by including obstacles' and road's PFs in the objective function of the optimal controller. It has the merits of both potential field and optimal control path planning techniques. In another word, it is able to consider any PF for obstacles and road structures while calculating the optimal path based on the obstacles, road structures, and vehicle dynamics. Other optimal control path planning systems usually consider the obstacles and road boundaries as constraints [10]–[13] or consider one cost function for all of them [14], and therefore, treat all of them in the same way despite their different characteristics. However, the proposed method allows considering different types for obstacles and road structures in the optimal control problem and treating them according to their characteristics. For instance, the presented autonomous vehicle passes a speed bump on its side when possible and cross it otherwise, while it stops behind a high profile stone if passing it on its side is not possible. Besides, the presented optimal control problem solves the two-dimensional obstacle avoidance problem through a quadratic model predictive controller, for which there are efficient algorithms solving the problem with lower computational cost than the existing algorithms for nonlinear model predictive controllers used in [13] and [14].

This paper is organized as follows. In Section II, the structure of an autonomous vehicle system and its different modules are presented, and the relationship between the path planning module and the other modules are explained. In Section III, the path planning problem, the vehicle dynamics model, and the PFs for different types of obstacles and road structure are defined, and the path planning optimal control problem is formulated. In Section IV, the path planning system is evaluated with a high fidelity CarSim simulation under several complicated scenarios, and the results are presented and discussed. Section V concludes the paper.

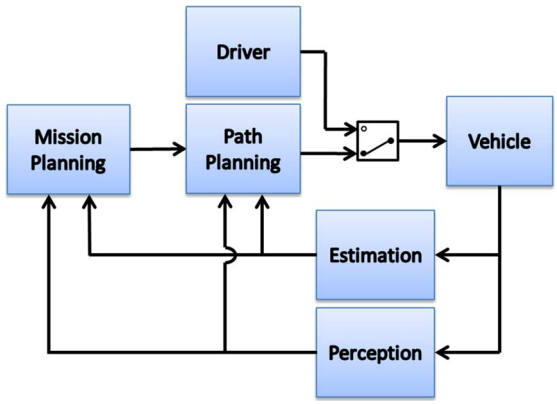


Fig. 1. Block diagram of the autonomous system.

## II. Overall Vehicle System

Even though this paper focuses on the path planning module in an autonomous vehicle system, there are more necessary modules, as shown in Fig. 1. In this paper, it is assumed that the path planning module receives the reference vehicle speed and the reference lane from the mission planning module. The mission planning module may generate these reference signals according to road regulations, planned vehicle route, and flows of the lanes [15]–[17]. The path planning module also receives the shape, position, and velocity of the obstacles, the road structure, and the regulations from the perception module [18]–[20], and the vehicle states from the estimation module [21]–[23]. The goal of the path planning module is to plan a path following the commands of the mission planning module while meeting the road regulations, avoiding the obstacles, and having a stable vehicle dynamics. The path planning module generates the front steering angle and the total longitudinal force commands. These choices of commands correspond to the driver commands, which include steering wheel angle and the gas/brake pedal positions, so that for a semi-autonomous vehicle, switching between the autonomous system and the driver can be performed simply. The path planning system is explained in the following section.

## III. Path Planning

This section presents a path planning system for autonomous road vehicles. First, a vehicle dynamics model is presented. Next, PFs for obstacles and road lane markers are defined. Then, the model predictive path planning problem is generated based on the vehicle model and PFs.

### A. Vehicle Dynamics Model

A bicycle model is used to model the vehicle dynamics. The notation used in the vehicle model is shown in Fig. 2. The

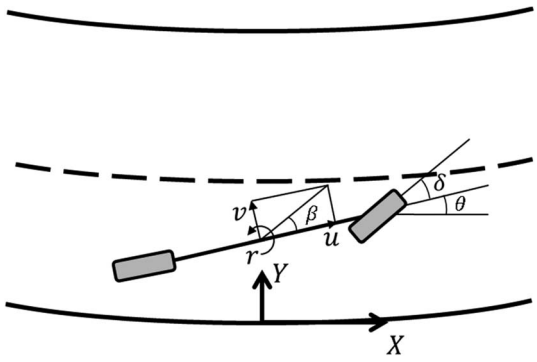


Fig. 2. Vehicle bicycle model.

equations of motion of the bicycle model are:

$$m(\dot{u} - vr) = F_{x_T} \tag{1}$$

$$m(\dot{v} + ur) = F_{y_f} + F_{y_r} \tag{2}$$

$$I_z \dot{r} = l_f F_{y_f} - l_r F_{y_r} \tag{3}$$

$$\dot{\theta} = r \tag{4}$$

$$\dot{X} = u\cos\theta - v\sin\theta \tag{5}$$

$$\dot{Y} = v\cos\theta + u\sin\theta \tag{6}$$

where $u$, $v$, and $r$ denote the longitudinal velocity, lateral velocity, and yaw rate of the vehicle at its center of gravity, $X$, $Y$ and $\theta$ are the longitudinal and lateral position and heading angle of the vehicle in the global coordinate, $F_{y_f}$ and $F_{y_r}$ are the total lateral forces of the front and rear tires, $F_{x_T}$ is the total longitudinal force of tires, $m$ is the vehicle's mass, and $I_z$ is the vehicle's momentum of inertia around its vertical axis.

The vehicle is assumed to have a front steering system. A linear tire model is used for the lateral tire forces [13]:

$$F_{y_f} = C_f \alpha_f = C_f \left(\delta - \frac{v + l_f r}{u}\right) \tag{7}$$

$$F_{y_r} = C_r \alpha_r = C_r \left(-\frac{v - l_r r}{u}\right) \tag{8}$$

in which $\alpha_f$ and $\alpha_r$ are the sideslip angles of the front and rear tires, and $\delta$ is the steering angle. Moreover, $C_f$ and $C_r$ denote the cornering stiffness values of the front and rear tires, respectively, which are obtained similar to [13].

The vehicle linear dynamics can then be obtained by linearizing (1)–(8) around the vehicle's operating point:

$$\dot{\boldsymbol{x}} = \boldsymbol{A}\boldsymbol{x} + \boldsymbol{B}\boldsymbol{u_c} \tag{9}$$

$$\boldsymbol{x} = [X \quad u \quad Y \quad v \quad \theta \quad r]^T \tag{10}$$

$$\boldsymbol{u_c} = [F_{x_T} \quad \delta]^T \tag{11}$$

where $\boldsymbol{x}$ is the state vector, $\boldsymbol{u_c}$ is the input vector, $\boldsymbol{A}$ is the state matrix, and $\boldsymbol{B}$ is the input matrix. The model is discretized by zero order hold method to be utilized as the model of the model predictive path planning controller.

### B. Potential Field

A potential field is a field generated by obstacle and goal PFs to lead the vehicle toward the goal while keeping it away from the obstacles. A goal PF has a minimum at the goal so that the goal attracts the vehicle, and an obstacle PF has a maximum at the obstacle position so that the obstacle repulses the vehicle. In this paper, the task of leading the vehicle towards its goal is performed by the tracking terms in the objective function of the path planning controller. Therefore, the potential field generated here is repulsive only, and is constructed of obstacle PFs. A PF is defined for the lane markers to prevent the vehicle from going out of its lane and the road $(U_{R_q})$. Two PFs are also defined for two categories of obstacles: obstacles that cannot be crossed like a vehicle $(U_{NC_i})$, and the one that can be crossed like a bump $(U_{C_j})$. The potential field is the sum of the PFs:

$$U = \sum_i U_{NC_i} + \sum_j U_{C_j} + \sum_q U_{R_q} \tag{12}$$

where indices $i$, $j$, and $q$ denote the $i$th non-crossable obstacle, the $j$th crossable obstacle, and the $q$th lane marker, respectively.

The presented functions below are some sample functions; other functions can be used for modeling other road regulations and obstacles. The presented method can handle any PF that is twice differentiable.

*1) Non-Crossable Obstacles:* Some obstacles should not be crossed since they are either important themselves like a pedestrian or can cause a damage to the vehicle, like a vehicle obstacle or a high profile object. A hyperbolic function of the distance between the vehicle and the obstacle is used to generate the potential field caused by this kind of obstacle. The rate of change of the function strictly increases as the distance to the obstacle position decreases, and it approaches to infinity, which prevents the vehicle from crossing the obstacle. Schulman *et al.* [24] uses the SD between the vehicle shape and the obstacle shape for collision avoidance. The SD is the minimum distance of the shapes if there is no contact between the shapes, or the negative of the penetration distance if there are contact points. More information on the signed distance can be found in [25]. The PF is generated as a function of the SD, $s_i$:

$$U_{NC_i}(X, Y) = \frac{a_i}{s_i\left(\frac{X}{X_{s_i}}, \frac{Y}{Y_{s_i}}\right)^{b_i}} \tag{13}$$

where $a_i$ and $b_i$ are intensity and shape parameters of the PF, respectively. In addition, the vehicle needs to have a larger distance to the obstacle in the longitudinal direction than the lateral direction. Therefore, the SD is normalized by the safe longitudinal and lateral distances from the obstacle, $X_{s_i}$ and $Y_{s_i}$, which are defined as:

$$X_{s_i} = X_0 + uT_0 + \frac{\Delta u_{a_i}^2}{2a_n} \tag{14}$$

$$Y_{s_i} = Y_0 + (u\sin\theta_e + u_{o_i}\sin\theta_e)\,T_0 + \frac{\Delta v_{a_i}^2}{2a_n}. \tag{15}$$

The safe longitudinal distance includes the minimum longitudinal distance, $X_0$, the distance spanned by the vehicle during the safe time gap, $T_0$, and the distance due to the longitudinal velocity difference between the vehicle and the obstacle [26]. The safe lateral distance includes the minimum lateral distance, $Y_0$, and the lateral distance spanned by the vehicle and the obstacle during the safe time gap if they have the constant heading angles of $\theta_e$ toward each other, and the distance due to the lateral velocity difference between the vehicle and the obstacle. The safe time gap compensates for the vehicle response time, and its value is assigned accordingly. Besides, $u_{o_i}$ is the longitudinal velocity of the $i$th obstacle, $a_n$ is the comfortable acceleration, and $\Delta u_{a_i}$ and $\Delta v_{a_i}$ are the approaching velocities in the longitudinal and lateral directions. In each direction, the approaching velocity is set to the velocity difference between the vehicle and the obstacle if they are approaching and to zero otherwise.

Moreover, zero SD results in an infinite PF. In addition, with this PF, the vehicle would have no longitudinal response to the obstacle approaches from the side, if the longitudinal component of the SD is zero, while a driver would brake in this situation. These issues are resolved with a modification in the calculation of the SD; if the longitudinal distance between the vehicle and the obstacle is less than a threshold, $\Delta X_0$, it is set to $\Delta X_0$ with the obstacle being ahead.

If the vehicle and the obstacle are approaching each other, there is a region around the obstacle where the vehicle cannot avoid a collision. The longitudinal and lateral collision distances, $X_{c_i}$ and $Y_{c_i}$, are defined as the maximum distances from the obstacle in the longitudinal and lateral directions at which the collision cannot be avoided. In each direction, the collision distance is the distance required to change the approaching velocity to zero by modifying the vehicle velocity with the maximum acceleration, $a_{\max}$:

$$X_{c_i} = \frac{\Delta u_{a_i}^2}{2a_{\max}} \tag{16}$$

$$Y_{c_i} = \frac{\Delta v_{a_i}^2}{2a_{\max}}. \tag{17}$$

The intensity and shape parameters of (13) are calculated by assigning the safe potential parameter, $U_{\text{saf}}$, and the accident potential parameter, $U_{\text{acc}}$, to the PF at the safe distance and the collision distance, respectively:

$$U_{NC_i} = \begin{cases} U_{\text{saf}} & s_i = 1 \\ U_{\text{acc}} & s_i = s_c. \end{cases} \tag{18}$$

It is notable that for being at the safe distance from the obstacle, the vehicle just needs to be at the safe distance in either lateral or longitudinal direction. The same expression holds for the collision distance. Therefore, the collision SD, $s_c$, is the maximum of the corresponding SD of the longitudinal collision distance and the corresponding SD of lateral collision distance. The potential field of an obstacle vehicle located at $(X_{o_i}, Y_{o_i}) = (20, 3.5)$ m and moving at the same speed as the vehicle at 80 Km/h is shown in Fig. 3.

*2) Crossable Obstacle:* Some obstacles can be crossed without any damage, but it is preferred not to cross them, if possible,

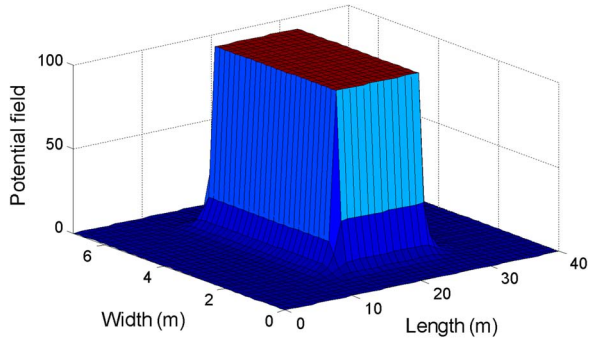


Fig. 3. Noncrossable obstacle potential field.

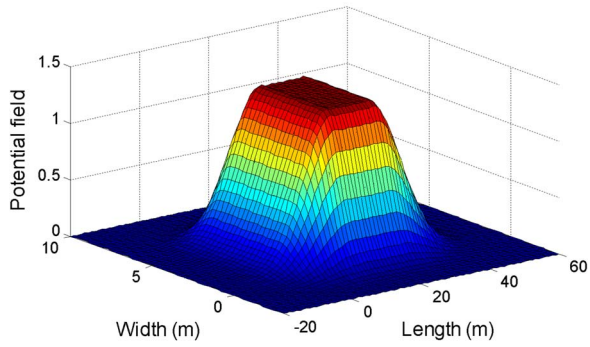


Fig. 4. Crossable obstacle potential field.

like a low profile object or a bump on the road. The PF of such an obstacle is defined with an exponential function:

$$U_{C_j}(X, Y) = a_j e^{-b_j s_j \left(\frac{X}{X_{s_j}}, \frac{Y}{Y_{s_j}}\right)} \tag{19}$$

where $s_j$ is the normalized SD between the vehicle and the obstacle calculated similar to (13)–(15). $a_j$ and $b_j$ are also the intensity and shape parameters, which are calculated similar to (14)–(18) except that the uncomfortable potential parameter, $U_{\text{unc}}$, is assigned to the PF at the collision distance.

The exponential function repulses the vehicle from the obstacle everywhere because of its positive gradient. But, at positions close to the obstacle, the gradient decreases as the distance to the obstacle decreases, which allows the vehicle to cross the obstacle. Fig. 4 shows the potential field generated by this function for a similar situation to that of Fig. 3.

*3) Road Lane Boundaries:* In a structured road, the vehicle should not cross the road lane markers unless a lane change is desired. To avoid undesirable lane marker crossings, PFs are defined for lane markers:

$$U_{R_q}(X, Y) = \begin{cases} a_q \left(s_{R_q}(X, Y) - D_a\right)^2 & s_{R_q}(X, Y) < D_a \\ 0 & s_{R_q}(X, Y) > D_a \end{cases} \tag{20}$$

where $s_{R_q}$ is the SD of the vehicle from the lane marker, $D_a$ is the allowed distance from the lane marker, index $q = r, l$ denotes the right or left lane marker, and $a_q$, is the intensity parameter calculated by assigning the lane marker potential parameter, $U_{\text{lma}}$, to the PF at zero SD.

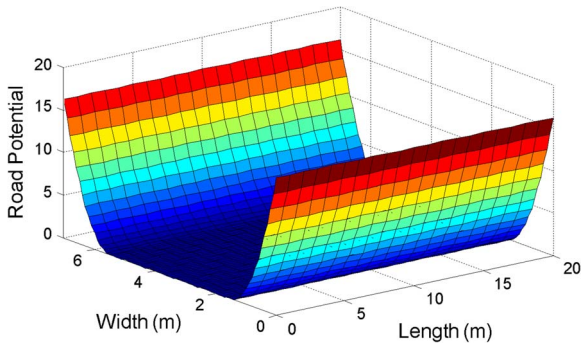


Fig. 5. Lane-changing road potential field.

If a lane keeping is intended, the right and left lane markers are the ones on which the PFs are implemented. If a lane change is intended, the PF is not implemented on the lane marker that can be crossed for the lane change. It is implemented on the next lane marker instead.

The lane marker PFs are defined with quadratic functions, and their gradients increase linearly as the SD decreases. Therefore, the vehicle can cross the lane markers to any extent, but the farther the vehicle goes from the middle of the lane the harder the PF pushes it toward there. Fig. 5 shows the road PF for a lane change maneuver on a two lane road.

### C. Path Planning

In this section, a model predictive path planning controller is developed with the presented vehicle dynamics model. The presented potential field for obstacles and road regulations is added to the controller objective to include the general obstacle avoidance and road regulation observation to the model predictive path planning system. With this objective, the path planning system has the vehicle dynamics consideration of an optimal control path planning method and the generality of a potential field method in considering different functions for the obstacles and road structures.

The model predictive controller predicts the response of the vehicle up to a horizon, and optimizes the vehicle dynamics, command following, obstacle avoidance, and road regulations observation up to that horizon based on the predicted values. For this optimal control problem, it is assumed that the desired lane and speed are predefined. Therefore, the desired lateral position, which is the center of the desired lane, and the desired longitudinal velocity are the outputs to be tracked:

$$\boldsymbol{y} = [Y \quad u]^T \tag{21}$$

$$\boldsymbol{y_{des}} = [Y_{\rm des} \quad u_{\rm des}]^T \tag{22}$$

$$Y_{\rm des} = \left(l_{\rm des} - \frac{1}{2}\right) L_w + \Delta Y_R \tag{23}$$

where $\boldsymbol{y}$ is the output matrix tracking the desired output matrix, $\boldsymbol{y_{des}}$, $Y_{\rm des}$ is the desired lateral position, $u_{\rm des}$ is the desired vehicle speed, $L_w$ is the lane width, $\Delta Y_R$ is the lateral offset of the road compared to a straight road, and $l_{\rm des}$ is the index number of the desired lane counted from the right.

There are some road regulations on the minimum and maximum speed limits that the vehicle should not violate. Moreover, since the tire longitudinal and lateral forces cannot exceed the friction ellipse, the model predictive controller should consider this limitation in its prediction to have an accurate prediction. Therefore, constraints are applied on the vehicle speed and tire forces to restrict their changes:

$$u_{\min} < u < u_{\max} \tag{24}$$

$$\left(\frac{F_{x_T}}{F_{x_T-\max}}\right)^2 + \left(\frac{F_{y_*}}{F_{y_*-\max}}\right)^2 < 1, \quad * = f, r \tag{25}$$

where $F_{x_T-\max}$ is the maximum total longitudinal tire force, $F_{y_*-\max}$, for $* = f, r$, is the maximum front or rear lateral tire force, and $u_{\min}$ and $u_{\max}$ are the minimum and maximum speed limits. In most cases, there is no minimum speed limit, so it is set to zero, and the desired speed is assigned to the maximum speed limit. It is notable that the constraints on the tire forces limit the sideslip angles to remain in intervals in which the tires' lateral forces behave almost linearly [13].

The constraints of (24) and (25) are applied in the optimal control problem as soft constraints. A soft constraint can be violated, but its violation is penalized. A slack variable is added to the constraint equation to allow some violation and constructs a penalty term in the objective function of the optimal control problem to penalize the violation. It is notable that although surpassing the tire ellipses is physically impossible, the constraints on the tire forces are considered soft to avoid possible feasibility issues due to errors in estimated vehicle states. Moreover, these constraints are quadratic and cannot be used in a quadratic optimal control problem. Each of the elliptical constraints is approximated by affine constraints through approximating the ellipse by an octagon inscribed in it.

The optimal control problem of the path planning is:

$$\min_{\boldsymbol{u_c},\boldsymbol{\varepsilon}} \sum_{k=1}^{N_p} U_{t+k,t} + \left\|\boldsymbol{y}_{t+k,t} - \boldsymbol{y_{des}}_{t+k,t}\right\|_{\boldsymbol{Q}}^2 + \left\|\boldsymbol{u_c}_{t+k-1,t}\right\|_{\boldsymbol{R}}^2 + \left\|\boldsymbol{u_c}_{t+k-1,t} - \boldsymbol{u_c}_{t+k-2,t}\right\|_{\boldsymbol{S}}^2 + \|\boldsymbol{\varepsilon}_k\|_{\boldsymbol{P}}^2 \tag{26}$$

s.t. $(k = 1, \ldots, N_p)$

$$\boldsymbol{x}_{t+k,t} = \boldsymbol{A_d}\boldsymbol{x}_{t+k-1,t} + \boldsymbol{B_d}\boldsymbol{u_c}_{t+k-1,t} \tag{27}$$

$$\boldsymbol{y}_{t+k,t} = \boldsymbol{C}\boldsymbol{x}_{t+k,t} + \boldsymbol{D}\boldsymbol{u_c}_{t+k,t} \tag{28}$$

$$\boldsymbol{y_s}_{t+k,t} = \boldsymbol{C_s}\boldsymbol{x}_{t+k,t} + \boldsymbol{D_s}\boldsymbol{u_c}_{t+k,t} \tag{29}$$

$$\boldsymbol{y_s}_{t+k,t} \le \boldsymbol{y_{s-\max}} + \boldsymbol{\varepsilon}_k \tag{30}$$

$$\boldsymbol{\varepsilon}_k \ge 0 \tag{31}$$

$$\boldsymbol{\varepsilon}_{k+1} = \boldsymbol{\varepsilon}_k, \quad k \ne c_1 N_{rs} + 1, \quad c_1 = 1, \ldots, N_p/N_{rs} \tag{32}$$

$$\boldsymbol{u_{c-\min}} < \boldsymbol{u_c}_{t+k-1,t} < \boldsymbol{u_{c-\max}} \tag{33}$$

$$\boldsymbol{\Delta u_{c-\min}} < \boldsymbol{u_c}_{t+k-1,t} - \boldsymbol{u_c}_{t+k-2,t} < \boldsymbol{\Delta u_{c-\max}} \tag{34}$$

$$\boldsymbol{u_c}_{t+k,t} = \boldsymbol{u_c}_{t+k-1,t}, \quad k > N_c, \quad k \ne c_2 N_{rc} + N_c, \quad c_2 = 1, \ldots, (N_p - N_c)/N_{rc} \tag{35}$$

$$\boldsymbol{u_c}_{t-1,t} = \boldsymbol{u_c}(t-1) \tag{36}$$

$$\boldsymbol{x}_{t,t} = \boldsymbol{x}(t) \tag{37}$$

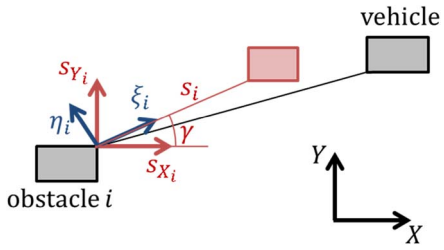


Fig. 6. Coordinate transformation.

where $t+k, t$ index denotes the predicted value at $k$ steps ahead of the current time $t$, $N_p$ is the prediction horizon, and $\boldsymbol{\varepsilon}_k$ is the vector of slack variables at $k$ steps ahead of the current time. The objective function includes the predicted potential field, and quadratic terms of tracking, inputs, changes in inputs, and slack variables with weighting matrices $\boldsymbol{Q}$, $\boldsymbol{R}$, $\boldsymbol{S}$, and $\boldsymbol{P}$, respectively. The states are predicted through (27), which is obtained by discretizing (9) to obtain $\boldsymbol{A_d}$ and $\boldsymbol{B_d}$ as the discrete state and input matrices. Equation (28) calculates the tracking outputs, where $\boldsymbol{C}$ and $\boldsymbol{D}$ are the output and feedforward matrices. The speed constraint (24) and the constraints of the octagon approximation of (25) are presented in (30), where $\boldsymbol{y_s}$ is the vector of soft constraint variables and is bounded by $\boldsymbol{y_{s-max}}$, the vector of constraint bounds, and the slack variable vector is included to allow violation of the bounds. The constraint variables are linearized around the operating point, to be written as a function of states and inputs in (29), where $\boldsymbol{C_s}$ and $\boldsymbol{D_s}$ are the output and feedforward matrices. The computation cost is reduced by reducing the number of slack variables and control inputs in (32) and (35). The slack variable vector changes every $N_{rs}$ prediction steps, and also after the first $N_c$ prediction steps, the control inputs change every $N_{rc}$ steps. The control inputs and their changes are also constrained in (33) and (34) to satisfy the actuator limitations, where $\boldsymbol{u_{c-min}}$ and $\boldsymbol{u_{c-max}}$ are the matrices of the lower and upper bounds of the control input, and $\boldsymbol{\Delta u_{c-min}}$ and $\boldsymbol{\Delta u_{c-min}}$ are the matrices of the lower and upper bounds of the control inputs changes.

The presented optimal control problem can be solved for any PF. However, because of the nonlinear nonconvex PFs, the problem is nonlinear and nonconvex, and its solution is expensive. Its approximated quadratic convex problem can be solved noticeably faster. Thus, to reduce the calculation time, the problem is converted into a quadratic convex problem. To do so, the PFs are first approximated by convex functions.

The PFs are defined on $(X, Y)$. Olfati-Saber [27] defines the obstacle PF only in the SD's direction to generate the repellant force. For each obstacle and at each prediction step, the PFs defined in this paper is transformed to a coordinate, $(\xi_i, \eta_i)$, that has one axis $(\xi_i)$ in the direction of the SD:

$$\begin{bmatrix}\xi_i \\ \eta_i\end{bmatrix} = \begin{bmatrix}\cos\gamma & \sin\gamma \\ -\sin\gamma & \cos\gamma\end{bmatrix}\begin{bmatrix}s_{X_i} \\ s_{Y_i}\end{bmatrix}. \tag{38}$$

Fig. 6 illustrates the coordinate transformation. The black coordinate is the road coordinate and the red coordinate is the SD coordinate, which is normalized with the safe distances. The red rectangle is the vehicle in this coordinate and $s_i$ is the SD. The vehicle position at the prediction step $k$ is anticipated based on the vehicle speed and heading angle at time step $t$. The angle between the SD at this position and $s_{x_i}$-axis is $\gamma$. The blue coordinate, $(\xi_i, \eta_i)$, is obtained by rotating the SD coordinate by this angle.

The PFs defined in Section III can all be written as a function of $s_i$ instead of $(X, Y)$. In other word, for a PF, $g : \mathbb{R}^2 \to \mathbb{R}$, there is a function, $h : \mathbb{R} \to \mathbb{R}$, that $h(s_i) = g(X, Y)$. Moreover, the PF, $g$, can be transformed from $(X, Y)$ to $(\xi_i, \eta_i)$ by (38) to obtain the transformed PF, $g_T : \mathbb{R}^2 \to \mathbb{R}$, where $g_T(\xi_i, \eta_i) = g(X, Y)$. Considering the definition of the SD, the gradient and Hessian of $g_T$ are:

$$s_i = \begin{cases} \left(\xi_i^2 + \eta_i^2\right)^{\frac{1}{2}} & \text{no contact} \\ -\left(-\xi_i^2 + \eta_i^2\right)^{\frac{1}{2}} & \text{in contact} \end{cases} \tag{39}$$

$$\nabla g_T = \begin{bmatrix} h'\frac{\xi_i}{s_i} & h'\frac{\eta_i}{s_i} \end{bmatrix}^T \tag{40}$$

$$\nabla^2 g_T = \begin{bmatrix} \frac{\xi_i^2}{s_i^2}h'' + \frac{s_i^2-\xi_i^2}{s_i^3}h' & \frac{\xi_i\eta_i}{s_i^2}h'' - \frac{\xi_i\eta_i}{s_i^3}h' \\ \frac{\xi_i\eta_i}{s_i^2}h'' - \frac{\xi_i\eta_i}{s_i^3}h' & \frac{\eta_i^2}{s_i^2}h'' + \frac{s_i^2-\eta_i^2}{s_i^3}h' \end{bmatrix} \tag{41}$$

where $h'$ and $h''$ are the first and second derivatives of function $h$ with respect to $s_i$. From (40) it can be seen that, at the anticipated vehicle position, the gradient is in $\xi_i$ direction, i.e. the repellant force is only in the direction of the SD, as it is in [27]. Moreover, due to (41), the Hessian matrix is uncorrelated at the anticipated vehicle position in the new coordinate. Therefore, the function is convex at this position if both diagonal elements are non-negative. If any diagonal element is negative, the function is linearized at the corresponding direction of the element, using the first order Taylor series. The resulting function is a convex function convexified around the anticipated operating point.

The convex function is then transformed to the original coordinate, $(X, Y)$. Since convexity holds for linear transformation, the transformed function is also a convex function. The whole process is equivalent to an eigenvalue decomposition process that only keeps the positive eigenvalues. Therefore, the Hessian of the resulted function is the closest positive definite matrix to the Hessian of the original function in terms of Frobenius norm [28].

The resulted convex function is then approximated by a quadratic function through the second order Taylor series. The quadratic function is a close convex quadratic approximation of the original function around the nominal point; its gradient equals the original function's gradient and its Hessian matrix is the closest positive definite matrix to the original function's Hessian matrix in terms of Frobenius norm. The quadratic approximation adds a calculation time spent on transformations, first and second derivatives, and Taylor series approximations. However, the added time is negligible compared to the calculation time of the optimization problems.

Using the resulted PFs, the optimal control problem is a convex quadratic optimization problem. The problem is similar to a corresponding nonlinear problem solved by Sequential Quadratic Programming (SQP) in one sequence. Boggs *et al.* [29] derives an upper bound for the optimization error of each

sequence of SQP, where the optimization error is the difference between the result of the sequence and the local minimum of the nonlinear problem in the neighborhood of the problem's initial value. Based on this upper bound, for the quadratic problem, the closer the problem's initial value is to the minimum, which is equivalent to the anticipated vehicle point being closer to the vehicle position at the minimum, the smaller the optimization error. Moreover, the closer the calculated Hessian matrices of the PFs to their Hessian matrices at the minimum, the smaller the optimization error. Therefore, a PF with a smaller convex quadratic approximation error and a smaller variation of Hessian matrix in the neighborhood of the problem's initial value result in a smaller optimization error. In the next section, the performance and the calculation time of the nonlinear problem and the quadratic problem are compared for a scenario. The other scenarios are simulated only for the quadratic problem.

## IV. Results

### A. Test Scenarios

Roads are dynamic environments with obstacles moving at different speeds in different lanes and positions. The roads themselves might be curved, and a lane might end or begin. Moreover, a vehicle might be required to change its lane or stay in the lane to take an exit or turn. For any combination of the obstacles, road, and intended lane, the undertaken maneuver might be different. In this paper, some test scenarios are defined to evaluate the performance of an autonomous driving system. Some normal scenarios for an autonomous driving system are:

- Lane keeping on curved roads
- Lane changing with no obstacle in the vicinity
- Keeping a desired distance from the vehicle in front of the ego vehicle (adaptive cruise control)

Other more complicated scenarios that an autonomous driving system should be able to perform include:

- Lane changing while there are vehicles on the intended lane
- Merging into a highway while there are vehicles on the right lane
- A vehicle carelessly approaching the ego vehicle from the side
- Non-crossable static obstacle on the lane
- Crossable static obstacle on the lane

The abovementioned complicated maneuvers are only some of the many cases that might happen when driving on a road. However, they can evaluate the performance of path planning systems in observing safety and road regulations. The first and second cases test the vehicle in observing safety and road regulations in a lane change. The vehicle should change the lane as soon as it is safe and keep its lane if it is not safe. In the second case, the current lane is ending and the vehicle may need to reduce its speed or even stop before the lane ends. The corresponding maneuvers of these situations include normal maneuvers such as lane changing and modifying speed to keep distance from the obstacles.

The third case tests the path planning system in predicting the lateral movement of the obstacles and taking action in emergency situations while observing the road regulations. The vehicle should be able to predict the obstacle's path and avoids the accident while keeping its lane, which is performed by keeping some space from the obstacle via accelerating or decelerating. It includes simple maneuvers such as lane keeping and keeping a safe distance from the obstacles.

The fourth and fifth cases test the path planning system for observation of the road regulations. The vehicle should keep its lane; if there is enough lateral space on the lane, it should pass the obstacle on the side; otherwise, it should stop behind the obstacle or cross it. It also tests the path planning system for differentiating different obstacles. In the situation that there is not enough lateral space for passing the obstacle on the side, if the obstacle is not crossable, the vehicle should stop behind it, and if it is crossable, the vehicle should cross it.

Altogether, these cases are appropriate for evaluating the performance of path planning systems in observing the safety and road regulations, obstacle avoidance, and longitudinal and lateral maneuverability. The following test scenarios are defined based on the above mentioned cases:

*Scenario 1*: The vehicle is merging to a highway and its lane ends in 150 m. It should change its lane from Lane 1 to Lane 2 while there are three vehicles on Lane 2. There is not enough space between these vehicles for the ego vehicle to merge safely between them.

*Scenario 2*: The vehicle starts on Lane 1 and is commanded to change its lane while there are three vehicles on Lane 2. There is enough space between these vehicles for the ego vehicle to go in between them. The road is curved with a radius of 300 m for $X = [200\ 250]$ m and a radius of $-300$ m for $X = [250\ 300]$ m.

*Scenario 3*: The vehicle starts on Lane 1 and is commanded to stay on Lane 1. There is a vehicle on Lane 2 on the same longitudinal position and with the same speed as the ego vehicle. It moves laterally from the center of Lane 2 towards the center of Lane 1 with a constant lateral velocity in the time interval of $t = [1\ 6]$ s. The ego vehicle should make enough space for it to avoid collision.

*Scenario 4*: The vehicle starts on Lane 1 and is commanded to stay on Lane 1. There is a static non-crossable obstacle on Lane 1 located at 0.5 m from the right boundary of the lane. The obstacle is assumed to be a square obstacle with 0.5 m length, and there is enough lateral space on the lane for the vehicle to pass it.

*Scenario 5*: The scenario is the same as Scenario 4 except that the obstacle is crossable.

*Scenario 6*: The scenario is the same as Scenario 4 except that the obstacle is located at 1.5 m from the right boundary of Lane 1, and therefore, there is not enough lateral space on the lane for the vehicle to pass the obstacle.

TABLE I
TEST SCENARIO PARAMETERS

| | $u_0$ $(Km/h)$ | $u_{des}$ $(Km/h)$ | $V_{o1}$ $(Km/h)$ | $V_{o2}$ $(Km/h)$ | $V_{o3}$ $(Km/h)$ | $X_{o01}$ $(m)$ | $X_{o02}$ $(m)$ | $X_{o03}$ $(m)$ |
|---|---|---|---|---|---|---|---|---|
| Scen. 1 | 100 | 100 | 100 | 100 | 100 | -40 | 0 | 40 |
| Scen. 2 | 80 | 100 | 100 | 100 | 100 | -25 | 0 | 25 |
| Scen. 3 | 80 | 80 | 80 | - | - | 0 | - | - |
| Scen. 4-7 | 80 | 80 | 0 | - | - | 80 | - | - |

TABLE II
CONTROLLER PARAMETERS

| Parameter | Value | Unit | Parameter | Value | Unit |
|---|---|---|---|---|---|
| $m$ | 2271 | $Kg$ | $D_a$ | 0.5 | $m$ |
| $I_z$ | 4600 | $Kg\ m^2$ | $F_{x_T-max}$ | 24800 | $N$ |
| $l_f$ | 1.421 | $m$ | $F_{y_f-max}$ | 10400 | $N$ |
| $l_r$ | 1.434 | $m$ | $F_{y_r-max}$ | 10600 | $N$ |
| $C_f$ | 132000 | $N$ | $N_p$ | 20 | - |
| $C_r$ | 136000 | $N$ | $N_c$ | 5 | - |
| $\Delta X_0$ | 1 | $m$ | $N_{rc}$ | 5 | - |
| $a_{max}$ | 9 | $m/s^2$ | $N_{rs}$ | 10 | - |
| $a_n$ | 1 | $m/s^2$ | $\boldsymbol{u_{min}}$ | $-[24800 \quad 0.2]$ | - |
| $T_0$ | 0.25 | $s$ | $\boldsymbol{u_{max}}$ | $[13000 \quad 0.2]$ | - |
| $\mu$ | 0.9 | - | $\boldsymbol{\Delta u_{min}}$ | $-[1600 \quad 0.02]$ | - |
| $L_w$ | 3.5 | $m$ | $\boldsymbol{\Delta u_{max}}$ | $[1600 \quad 0.02]$ | - |
| $U_{saf}$ | 1 | - | $\boldsymbol{Q}$ | $[0.2 \quad 0.01]$ | - |
| $U_{acc}$ | 10 | - | $\boldsymbol{R}$ | $[2e-9 \quad 100]$ | - |
| $U_{unc}$ | 2 | - | $\boldsymbol{S}$ | $[5e-8 \quad 500]$ | - |
| $U_{lma}$ | 2 | - | | | |

*Scenario 7*: The scenario is the same as Scenario 6 except that the obstacle is crossable.

The initial vehicle speed, $u_0$, the desired vehicle speed. $u_{\mathrm{des}}$, the speed of obstacle(s), $u_{oi}$, and initial position of the obstacle(s) relative to the vehicle, $X_{o0i}$, are listed in Table I.

### B. Simulation

The proposed path planning controller is simulated on a vehicle system to evaluate the performance of the controller. The vehicle system used in the simulation is a model of a Chevrolet Equinox in CarSim software. The vehicle parameters used in the path planning controller are extracted from this vehicle model. The controller parameters are shown in Table II for a dry road. The vehicle is an electric vehicle with four wheel electric motors. It is notable that, the longitudinal tire force calculated by the path planning controller is applied through the wheel motors and the brakes. The motor torque and brake torque that generates a quarter of the force are calculated and applied to each wheel. The upper and lower bounds on the longitudinal force in the table are based on the tires' forces and motors' and brakes' torques capacities at the vehicle speed of 80 Km/h. In this section, the controller is simulated for the scenarios presented in the previous section so that its performance in observing the road regulations, obstacle avoidance, and maneuverability is evaluated. The controller time step is 50 ms.

Scenarios 1 is a merging maneuver when there are moving obstacles on the other lane and the current lane is ending. The scenario is simulated for the nonlinear and quadratic path planning problems, and the simulation results are shown in Fig. 7. The paths of the ego vehicle and obstacles are shown in Fig. 7(a). In this figure, at some sample times, markers are used to demonstrate the position of the vehicle and obstacles; each shape represents a sample time, and each color represents each of the vehicle or obstacles. As it is shown, the vehicle waits for all the obstacles to pass; the potential fields of the obstacles keep the vehicle away from Lane 2 when there are obstacles occupying it. Moreover, a potential field of a static obstacle located at the end of Lane 1 is added to the existing potential field to keep the vehicle from passing the end of the lane. Due to this potential field, the vehicle reduces its speed and avoids passing the end of the lane. After all the obstacles pass, the vehicle changes its lane safely. At the end of the lane change, the potential field of the left lane boundary keeps the vehicle from going out of the road.

The scenario is simulated for the nonlinear and quadratic problems. As it can be seen, the quadratic path planning system imitates the behavior of the nonlinear path planning system. The difference between the simulation results is only noticed closer to the end of the lane. At this location, the required large deceleration causes an error in the anticipated longitudinal vehicle position. Moreover, since the anticipated vehicle position is too close to the end of the lane, the error in approximating the hyperbolic PF of the end of the lane by a quadratic convex function becomes more noticeable. These two sources cause the differences in the results of the quadratic problem. Despite the differences, the performance of the quadratic problem is comparable to that of the nonlinear problem. On the other hand, the average calculation time of the nonlinear problem for a time step of this simulation is 21.03 s while that of the quadratic problem is 0.0094 s. It is notable that since the step time is 0.05 s, the quadratic problem can be solved in real time. The other scenarios are simulated for the quadratic problem.

Scenario 2 is a lane change while there are moving obstacles on the intended lane. Fig. 8 shows the simulation results for this scenario. Since there is a moving obstacle on the vehicle's side, the vehicle cannot proceed with the lane change immediately; the potential fields of the obstacles keep the vehicle away from Lane 2. The vehicle slightly reduces its speed, and waits for the obstacle on its side to pass. When there is enough distance to the obstacles in front and behind of the vehicle, it moves to the other lane while keeping its distance from the both obstacles by adjusting its speed. The lateral movements of the vehicle and its speed changes are according to the PFs keeping the vehicle away from the obstacles. It can also be seen that the path planning system can handle the maneuvers on a curved road.

In this scenario, the vehicle merges in between the obstacles since there is enough space. In Scenario 1, there was less space between the obstacles and also the vehicle's speed was largely different from obstacles' speeds. Therefore, going in between the obstacles was not safe enough and the potential fields of the obstacles kept the vehicle in Lane 1 until all the obstacles passed the vehicle and the lane change was safe.

The third scenario is when a moving obstacle beside the vehicle carelessly changes its lane to the vehicle's current lane. The simulation results for Scenario 3 are shown in Fig. 9. Due to the potential field of the obstacle, the vehicle reduces its speed to make some space for the obstacle, and moves to the right to keep its lateral distance from the obstacle and avoid collision. The potential field of the right boundary lane, on the other hand, leads the vehicle towards the middle of the lane

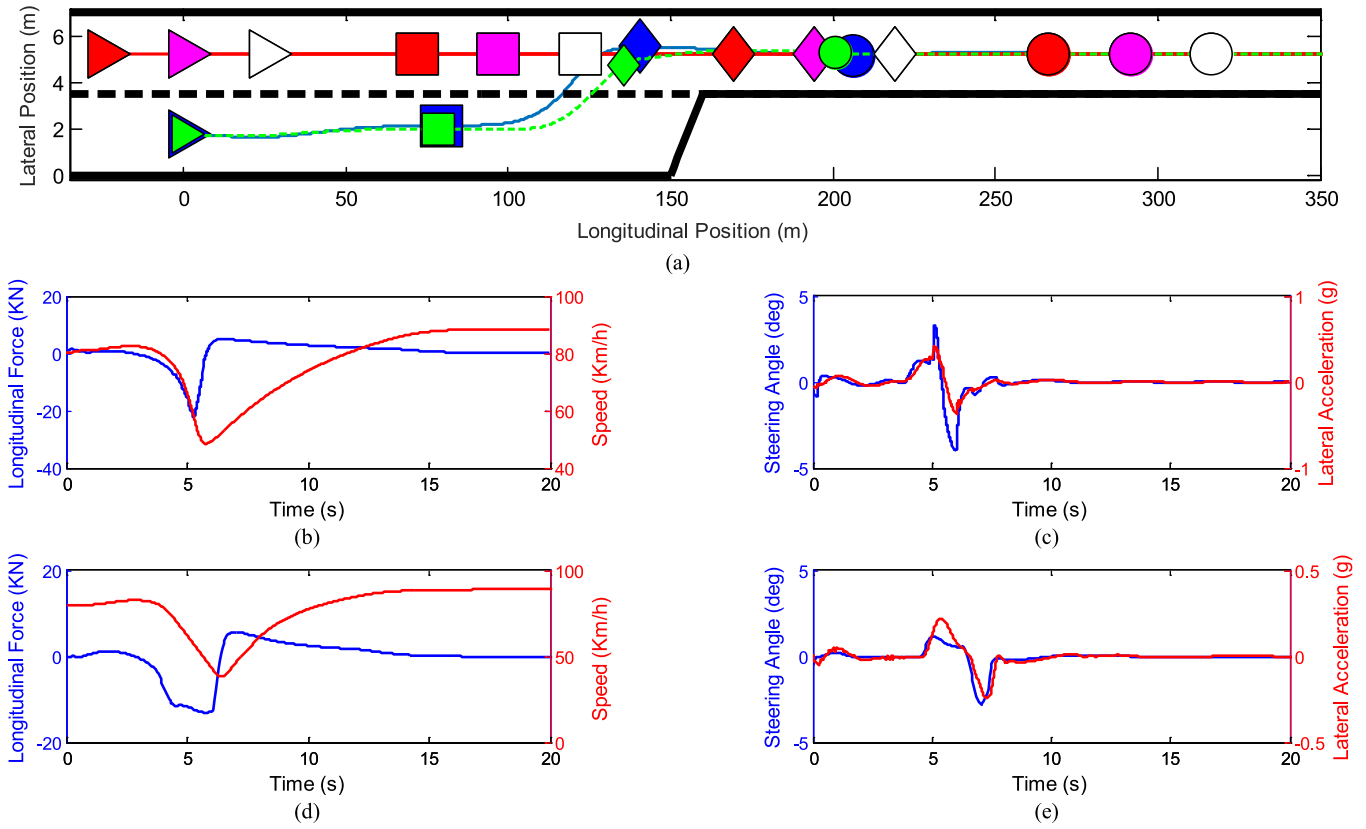


Fig. 7. Scenario 1 for nonlinear and quadratic problems. (a) Paths of vehicle and obstacles: (blue) vehicle for nonlinear problem; (green) vehicle for quadratic problem; (red) Obstacle 1; (purple) Obstacle 2; (white) Obstacle 3. (b) Longitudinal force command and vehicle speed for nonlinear problem. (c) Steering angle command and lateral acceleration for nonlinear problem. (d) Longitudinal force command and vehicle speed for quadratic problem. (e) Steering angle command and lateral acceleration for quadratic problem.

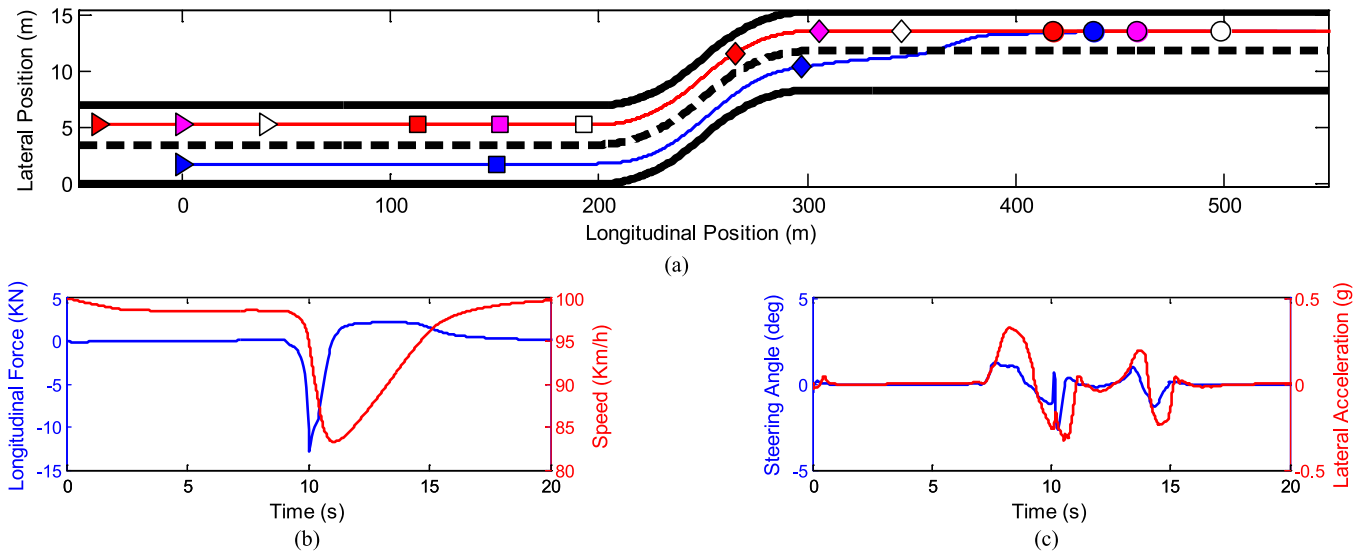


Fig. 8. Scenario 2. (a) Paths of vehicle and obstacles: (blue) vehicle; (red) Obstacle 1; (purple) Obstacle 2; (white) Obstacle 3. (b) Longitudinal force command and vehicle speed. (c) Steering angle command and lateral acceleration.

and keeps the vehicle in the lane. By the time the obstacle is on the middle lane marker, the vehicle has made around 10 m longitudinal space to make a safe distance with the obstacle. The vehicle goes back towards the center of the lane, due to the right lane boundary PF, after making enough longitudinal space for obstacle avoidance.

Scenarios 4–7 are designed to show different responses of the path planning system to different kinds of obstacles. Two kinds of obstacles are considered: crossable obstacles and non-crossable obstacles. Scenarios 4 and 5 are when there is a crossable or non-crossable obstacle on the current lane of the vehicle, but there is enough lateral space to pass the obstacle on

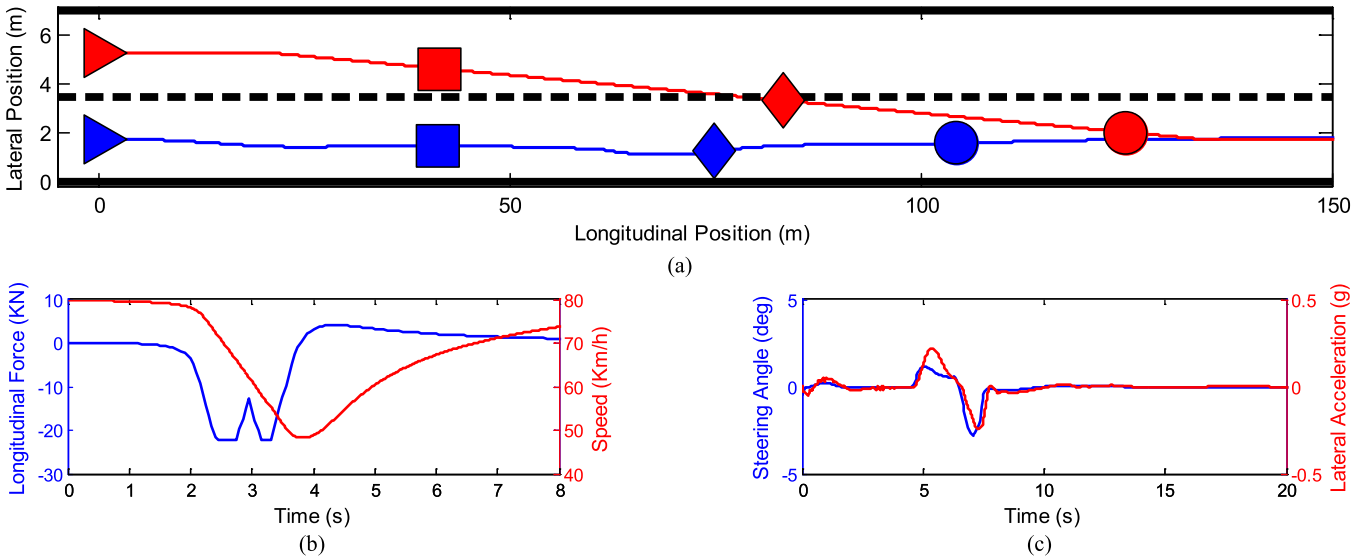


Fig. 9. Scenario 3. (a) Paths of vehicle and obstacle: (blue) vehicle; (red) obstacle. (b) Longitudinal force command and vehicle speed. (c) Steering angle command and lateral acceleration.

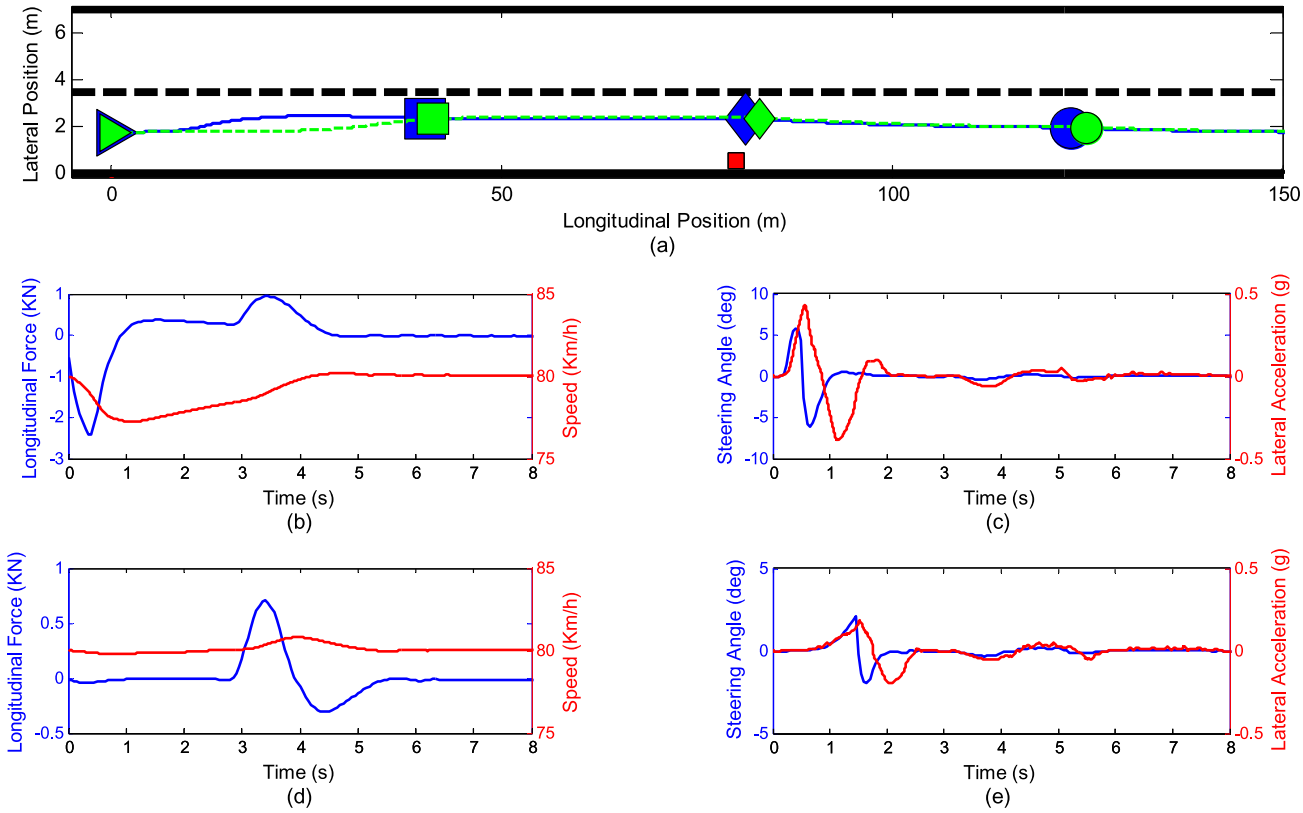


Fig. 10. Scenarios 4 and 5. (a) Vehicle's path and obstacles' position: (blue) vehicle of Scenario 4; (purple) vehicle of Scenario 5; (red) obstacle. (b) Longitudinal force command and vehicle speed in Scenario 4. (c) Steering angle command and lateral acceleration in Scenario 4. (d) Longitudinal force command and vehicle speed in Scenario 5. (e) Steering angle command and lateral acceleration in Scenario 5.

the side. The simulation results for these scenarios are shown in Fig. 10. The PFs of the obstacles lead the vehicle to the left of the lane, and the road potential field leads the vehicle to the right. As a result, the vehicle moves slightly to the left to pass the obstacle while it stays on the lane. At the time that the vehicle passes the obstacle, the lateral distance between the boundary of the obstacle and that of the vehicle is around 0.6 m for both Scenarios 4 and 5. After the vehicle passes the obstacle, the road potential field leads the vehicle back to the lane center. Moreover, the vehicle speed does not change noticeably in any of the cases, as expected. It is notable that the obstacle of Scenario 4 is static, and therefore, its potential field is sharper, which lets the vehicle passes it on the side with a smaller margin.

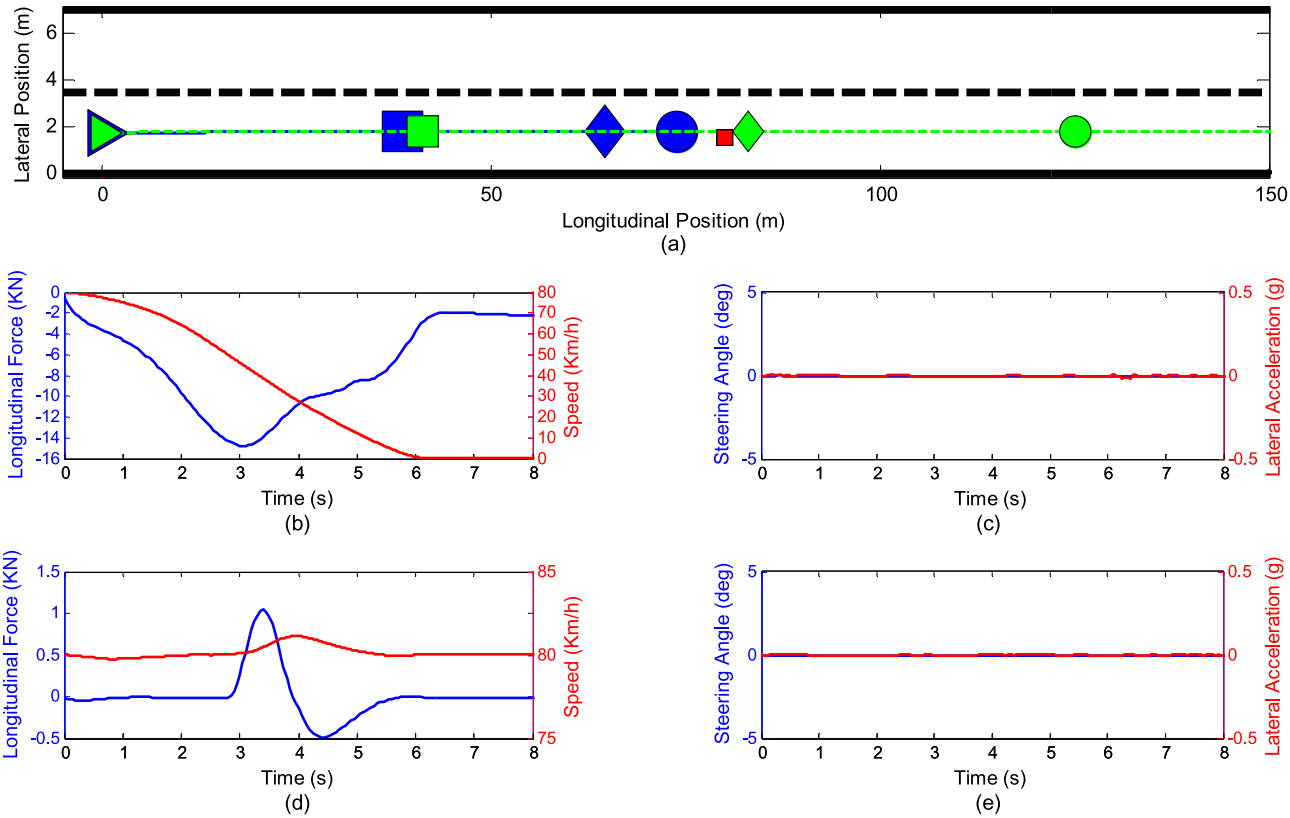


Fig. 11. Scenarios 6 and 7. (a) Vehicle's path and obstacle's position: (blue) vehicle of Scenario 6; (purple) vehicle of Scenario 7; (red) obstacle. (b) Longitudinal force command and vehicle speed in Scenario 6. (c) Steering angle command and lateral acceleration in Scenario 6. (d) Longitudinal force command and vehicle speed in Scenario 7. (e) Steering angle command and lateral acceleration in Scenario 7.

Scenarios 6 and 7 are where there is a crossable or non-crossable obstacle on the current lane of the vehicle, and there is not enough lateral space to pass the obstacle on the side. The simulation results of these scenarios are shown in Fig. 11. As the results show, the potential field of the non-crossable obstacle leads the vehicle to stop behind the obstacle. The crossable obstacle, however, is crossed while the vehicle does not change its speed considerably, showing the appropriate choice of the crossable obstacle PF. Moreover, for both cases, the vehicle does not move noticeably in the lateral direction.

## V. Conclusion

In this paper, a model predictive path planning controller was introduced utilizing potential field concept for its obstacle avoidance. Model predictive path planning controllers predict the vehicle dynamics and generate the optimal path based on the vehicle dynamics. They usually consider obstacles and road regulations as constraints, which although guarantees an obstacle avoidance, limits their capability in considering different kinds of obstacles and road structures. Potential field path planning methods, on the other hand, can consider different PFs for different obstacles and road structures, but they do not consider vehicle dynamics in path planning. The combination of these two methods is used in this paper, which can have the advantage of both considering different PFs for different obstacles and road structures and having feasible maneuverability due to predicting vehicle dynamics. In addition, appropriate choice of parameters of a PF can provide enough potential force to avoid an obstacle. Therefore, even for the obstacles that must be avoided, a PF is advantageous over an obstacle avoidance constraint; it not only avoids the obstacle, but also keeps the vehicle at an appropriate distance from the obstacle. The conditions guaranteeing obstacle avoidance of a PF can be studies in future works.

Different PFs were presented for crossable and non-crossable obstacles, and road lane markers. A model predictive path planning controller with a vehicle dynamics model was considered to follow the mission planning commands including the desired speed and commanded lane. The potential field was included in the controller's objective for obstacle avoidance and observing road regulations.

The optimal control problem is nonlinear and to reduce the computational time, the problem was approximated by a quadratic convex problem. The calculation time and the performance of the nonlinear and quadratic problems were compared by simulation. The results showed that although the approximation can cause errors in the result of the quadratic problem, the performance of the quadratic problem was acceptable with a fraction of time needed to solve the nonlinear problem. Further investigations should be performed on the range of validity of the approximation.

Some complex test scenarios were defined to evaluate the performance of the proposed path planning controller. The simulations were using high fidelity vehicle models in CarSim, although the vehicle model of the path planning controller was

a linear bicycle model. The results showed the capability of the introduced path planning method in preforming appropriate maneuvers in complicated scenarios. When a lane change is commanded from the mission planning module, the vehicle does not change its lane unless it is safe to do so. The vehicle merges in between two vehicles if there is enough space between them and it is safe to merge. If the current lane is ending, and a lane change is not safe, the vehicle reduces its speed or even stops before the lane ends, and changes its lane only when it is safe to do so. If a vehicle is approaching the vehicle from the side carelessly, the vehicle makes space for it as much as possible while staying on the road. Moreover, an advantage of the proposed method is treating different kinds of obstacles differently. If an obstacle is not crossable and there is not enough space on the side to pass, the vehicle stops behinds it. On the other hand, if an obstacle is crossable and there is not enough space on the side to pass, the vehicle crosses the obstacle. For both kinds of obstacles, the vehicle passes them on the side, if possible. For all these different complicated scenarios, potential fields keep the vehicle away from the obstacles and road boundaries, and the tracking terms of the objective functions guide the vehicle toward their desired speed and lane.

The proposed path planning method is capable of including different obstacles and road structures in the optimal control problem with different PFs to include importance and priorities. Moreover, since the vehicle dynamics is used as the prediction model, the planned path is the optimal path in terms of vehicle dynamics.

## ACKNOWLEDGMENT

The authors would like to acknowledge the technical support of General Motors Co.

## REFERENCES

[1] "Critical reasons for crashes investigated in the national motor vehicle crash causation survey," Nat. Highway Traffic Safety Admin., Washington, DC, USA, DOT HS 812 115, Feb. 2015.
[2] S. Karaman and E. Frazzoli, "Sampling-based algorithms for optimal motion planning," *Int. J. Robot. Res.*, vol. 30, no. 7, pp. 846–894, 2011.
[3] C. Goerzen, Z. Kong, and B. Mettler, "A survey of motion planning algorithms from the perspective of autonomous UAV guidance," *J. Intell. Robot. Syst.*, vol. 57, no. 1–4, pp. 65–100, 2010.
[4] D. Dolgov, S. Thrun, and M. Montemerlo, "Path planning for autonomous vehicles in unknown semi-structured environments," *Int. J. Robot. Res.*, vol. 29, no. 5, pp. 485–501, 2010.
[5] J. Wang, J. Wu, and Y. Li, "The driving safety field based on driver–vehicle–road interactions," *IEEE Trans. Intell. Transp. Syst.*, vol. 16, no. 4, pp. 2203–2214, Aug. 2015.
[6] M. T. Wolf and J. W. Burdick, "Artificial potential functions for highway driving with collision avoidance," in *Proc. IEEE ICRA*, 2008, pp. 3731–3736.
[7] J. Jia, A. Khajepour, W. Melek, and Y. Huang, "Path planning and tracking for vehicle collision avoidance based on model predictive control with multi-constraints," *IEEE Trans. Veh. Technol.*, [Online]. Available: http://ieeexplore.ieee.org/document/7458179/
[8] S. M. Erlien, "Shared vehicle control using safe driving envelopes for obstacle avoidance and stability," Ph.D. dissertation, Dept. Mech. Eng., Stanford Univ., Stanford, CA, USA, 2015.
[9] N. Noto, H. Okuda, and Y. Tazaki, "Steering assisting system for obstacle avoidance based on personalized potential field," in *Proc. IEEE 15th ITSC*, 2012, pp. 1702–1707.
[10] G. Schildbach and F. Borrelli, "Scenario model predictive control for lane change assistance on highways," in *Proc. IEEE IV*, 2015, pp. 611–616.
[11] A. Carvalho, Y. Gao, and S. Lefevre, "Stochastic predictive control of autonomous vehicles in uncertain environments," in *Proc. 12th Int. Symp. Adv. Veh. Control*, 2014, pp. 1–8.
[12] A. Carvalho, S. Lefévre, and G. Schildbach, "Automated driving: The role of forecasts and uncertainty—A control perspective," *Eur. J. Control*, vol. 24, pp. 14–32, 2015.
[13] Y. Gao, A. Gray, and H. E. Tseng, "A tube-based robust nonlinear predictive control approach to semiautonomous ground vehicles," *Veh. Syst. Dyn.*, vol. 52, no. 6, pp. 802–823, 2014.
[14] Y. Gao, T. Lin, F. Borrelli, E. Tseng, and D. Hrovat, "Predictive control of autonomous ground vehicles with obstacle avoidance on slippery roads," in *Proc. ASME Dyn. Syst. Control Conf.*, 2010, pp. 265–272.
[15] S. Glaser, B. Vanholme, and S. Mammar, "Maneuver-based trajectory planning for highly autonomous vehicles on real road with traffic and driver interaction," *IEEE Trans. Intell. Transp. Syst.*, vol. 11, no. 3, pp. 589–606, Sep. 2010.
[16] M. Ardelt, C. Coester, and N. Kaempchen, "Highly automated driving on freeways in real traffic using a probabilistic framework," *IEEE Trans. Intell. Transp. Syst.*, vol. 13, no. 4, pp. 1576–1585, Apr. 2012.
[17] J. Nilsson and J. Sjoberg, "Strategic decision making for automated driving on two-lane, one way roads using model predictive control," in *Proc. IEEE IV*, 2013, pp. 1253–1258.
[18] A. Mukhtar, L. Xia, and T. B. Tang, "Vehicle detection techniques for collision avoidance systems: A review," *IEEE Trans. Intell. Transp. Syst.*, vol. 16, no. 5, pp. 2318–2338, Oct. 2015.
[19] N. Kumar, J. Lee, and J. J. Rodrigues, "Intelligent mobile video surveillance system as a Bayesian coalition game in vehicular sensor networks: Learning automata approach," *IEEE Trans. Intell. Transp. Syst.*, vol. 16, no. 3, pp. 1148–1161, Jun. 2015.
[20] H. Guan, J. Li, and Y. Yu, "Using mobile LiDAR data for rapidly updating road markings," *IEEE Trans. Intell. Transp. Syst.*, vol. 16, no. 5, pp. 2457–2466, Oct. 2015.
[21] R. Zarringhalam, A. Rezaeian, and S. Fallah, "Optimal sensor configuration and fault-tolerant estimation of vehicle states," *SAE Int. J. Passenger Cars-Electron. Electr. Syst.*, vol. 6, no. 1, pp. 83–92, 2013.
[22] S. Miura, L. Hsu, and F. Chen, "GPS error correction with pseudorange evaluation using three-dimensional maps," *IEEE Trans. Intell. Transp. Syst.*, vol. 16, no. 6, pp. 3104–3115, Dec. 2015.
[23] K. Jo, M. Lee, and M. Sunwoo, "Road slope aided vehicle position estimation system based on sensor fusion of GPS and automotive onboard sensors," *IEEE Trans. Intell. Transp. Syst.*, vol. 17, no. 1, pp. 250–263, Jan. 2016.
[24] J. Schulman, J. Ho, and A. X. Lee, "Finding locally optimal, collision-free trajectories with sequential convex optimization," in *Proc. Robot. Sci. Syst.* 2013, vol. 9, pp. 1–10.
[25] C. Ericson, *Real-Time Collision Detection*. Boca Raton, FL, USA: CRC Press, 2004.
[26] A. Kesting, M. Treiber, and M. Schönhof, "Adaptive cruise control design for active congestion avoidance," *Transp. Res. C, Emerg. Technol.*, vol. 16, no. 6, pp. 668–683, 2008.
[27] R. Olfati-Saber, "Flocking for multi-agent dynamic systems: Algorithms and theory," *IEEE Trans. Autom. Control*, vol. 51, no. 3, pp. 401–420, Mar. 2006.
[28] M. Tanaka and K. Nakata, "Positive definite matrix approximation with condition number constraint," *Optim. Lett.*, vol. 8, no. 3, pp. 939–947, 2014.
[29] P. T. Boggs and J. W. Tolle, "Sequential quadratic programming," *Acta Numerica*, vol. 4, pp. 1–51, 1995.

**Yadollah Rasekhipour** received the B.Sc. and M.Sc. degrees in mechanical engineering from Amirkabir University of Technology, Tehran, Iran, in 2009 and 2012, respectively. He is currently working toward the Ph.D. degree in mechanical engineering at University of Waterloo, Waterloo, ON, Canada.

His research interests include autonomous vehicles, vehicle dynamics and control, noise, vibration and harshness of vehicles, suspension systems and engine mounting systems, and advanced control methods and their real-time applications.

**Amir Khajepour** received the B.S. degree from Ferdowsi University in 1990; the M.S. degree from Sharif University of Technology in 1992; and the Ph.D. degree from University of Waterloo in 1996.

He is a Professor of mechanical and mechatronics engineering with University of Waterloo, Waterloo, ON, Canada, where he is also the Canada Research Chair in Mechatronic Vehicle Systems. He has developed an extensive research program that applies his expertise in several key multidisciplinary areas. He has authored over 350 journal and conference publications and five books. His research interests include system modeling and control of dynamic systems. His research has resulted in several patents and technology transfers.

Prof. Khajepour is a Fellow of The Engineering Institute of Canada, The American Society of Mechanical Engineers, and The Canadian Society of Mechanical Engineering.

**Shih-Ken Chen** received the B.S. degree from National Taiwan University, Taipei, Taiwan, in 1985; the M.S. degree in mechanical engineering from University of Wisconsin–Madison, Madison, WI, USA, in 1990; and the Ph.D. degree in mechanical engineering from Massachusetts Institute of Technology, Cambridge, MA, USA, in 1996.

He was with the Research and Development Center of General Motors (GM) Corporation. He is currently a Staff Researcher with the Global R&D Center, GM, Warren, MI, USA. His previous research interests include collision-avoidance systems, electronic stability control, active all-wheel-steer control, and rollover avoidance. His current research interests include integrated chassis and vehicle control for both conventional and electric drivelines, driver-in-the-loop vehicle control, and vehicle active safety systems.

**Bakhtiar Litkouhi** received the B.S. degree in mechanical engineering from Sharif University of Technology in 1977; M.S. degree in applied mathematics, and the Ph.D. degree in systems science, specializing in controls, from Michigan State University in 1979 and 1983, respectively.

He was an Assistant Professor with Oakland University, Rochester, MI, USA. He was the Acting Director with the Electrical and Controls Integration Laboratory, Global Research and Development Center, General Motors Company, Warren, MI. He was a Program Manager for several large-scale projects on intelligent vehicle systems, human–machine faces, systems engineering, and integrated vehicle control, where he has made many contributions through numerous patents, publications, and presentations. He is currently the Manager of perception and vehicle control systems with the Global Research and Development Center. He is also a Program Manager with General Motors and Carnegie Mellon University Autonomous Driving Collaborative Research Laboratory, Pittsburgh, PA, USA, and a member of the Board of Directors with Waterloo Center for Automotive Research.

Dr. Litkouhi is a Board Member of the Intelligent Transportation Society of Michigan.